Pattern Recognition Letters 32 (2011) 120–126

Contents lists available at ScienceDirect

Pattern Recognition Letters

journal homepage: www.elsevier.com/locate/patrec

Empirical study of light source selection for palmprint recognition

Zhenhua Guo [a], David Zhang [b,*], Lei Zhang [b], Wangmeng Zuo [c], Guangming Lu [d]

[a] Graduate School at Shenzhen, Tsinghua University, Shenzhen, China
[b] Department of Computing, The Hong Kong Polytechnic University, Kowloon, Hong Kong
[c] School of Computer Science and Technology, Harbin Institute of Technology, Harbin, China
[d] Shenzhen Graduate School, Harbin Institute of Technology, Shenzhen, China

ARTICLE INFO

Article history:
Received 1 December 2009
Available online 8 October 2010
Communicated by G. Borgefors

Keywords:
Biometrics
Palmprint recognition
Illumination
Orientation code

ABSTRACT

Most of the current palmprint recognition systems use an active light to acquire images, and the light source is a key component in the system. Although white light is the most widely used light source, little work has been done on investigating whether it is the best illumination for palmprint recognition. This study analyzes the palmprint recognition performance under seven different illuminations, including the white light. The experimental results on a large database show that white light is not the optimal illumination, while yellow or magenta light could achieve higher palmprint recognition accuracy than the white light.

1. Introduction

Automatic authentication using biometric characteristics, as a replacement or complement to traditional personal authentication, is becoming more and more popular in the current e-world. Biometrics is the study of methods for uniquely recognizing humans based on one or more intrinsic physical or behavioral traits, such as face, iris, fingerprint, signature, gait and finger-knuckle-print (Jain et al., 1999; Zhang et al., 2010). As an important member of the biometric characteristics, palmprint has merits such as robustness, user-friendliness, high accuracy, and cost-effectiveness. Because of these good properties, palmprint recognition has been receiving a lot of research attention and many palmprint systems have been proposed (Connie et al., 2005; Duta et al., 2002; Han, 2004; Han et al., 2007; Kumar et al., 2003; Lin et al., 2005; Michael et al., 2008; Ribaric and Fratric, 2005; Wang et al., 2008; Wu et al., 2008; Zhang et al., 2003; Zhang and Shu, 1999).

In the early stage, most works focus on offline palmprint images (Duta et al., 2002; Zhang and Shu, 1999). With the development of digital image acquisition devices, many online palmprint systems have been proposed (Connie et al., 2005; Han, 2004; Han et al., 2007; Kumar et al., 2003; Lin et al., 2005; Michael et al., 2008; Ribaric and Fratric, 2005; Wang et al., 2008; Wu et al., 2008; Zhang et al., 2003). Based on the sensors used, online palmprint image acquisition systems can be grouped into four types (Kong et al., 2009): digital scanners (Connie et al., 2005; Lin et al., 2005; Ribaric and Fratric, 2005), video cameras (Han et al., 2007; Michael et al., 2008), CCD (Charge Coupled Device) based palmprint scanner (Han, 2004; Wang et al., 2008; Zhang et al., 2003) and digital cameras (Kumar et al., 2003; Wu et al., 2008). On the other hand, according to imaging conditions, these systems could be classified into three classes: digital scanners (Connie et al., 2005; Lin et al., 2005; Ribaric and Fratric, 2005), camera with passive illumination (Han et al., 2007; Kumar et al., 2003; Wang et al., 2008), and camera with active illumination (Han, 2004; Michael et al., 2008; Wu et al., 2008; Zhang et al., 2003).

Desktop scanner could provide high quality palmprint images (Connie et al., 2005; Lin et al., 2005; Ribaric and Fratric, 2005) under different resolutions. However, it suffers from the slow scanning speed (Kong et al., 2009) and it requires the full touch of whole hand, which may bring sanitary issues during data collection. Using camera with uncontrolled ambient lighting (Han et al., 2007; Kumar et al., 2003; Wang et al., 2008) does not have the above problems. However, the image quality may not be very good as the illumination lighting may change much so that the recognition accuracy can be reduced. Because camera mounted with active light could collect image data quickly with good image quality and it does not require the full touch with the device, this kind of systems have been widely adopted (Han, 2004; Michael et al., 2008; Wu et al., 2008; Zhang et al., 2003). In these systems, the light source is a key component and there are some principles on the setting of lighting scheme (Wong et al., 2005). In spite of the fact that all these studies (Han, 2004; Michael et al., 2008; Wu et al., 2008; Zhang et al., 2003) use white light source for palmprint imaging, little work has been done to systematically validate whether white light is the optimal light. Our previous work (Guo et al., 2009) showed that white light may not be the optimal one for palmprint

* Corresponding author. Tel.: +852 27667271; fax: +852 27740842.
E-mail address: csdzhang@comp.polyu.edu.hk (D. Zhang).

0167-8655/$ - see front matter © 2010 Elsevier B.V. All rights reserved.
doi:10.1016/j.patrec.2010.09.026

recognition, but the finding may be biased as the study is limited by using only one recognition method. Furthermore, the underlying principle is not explored. To this end, this study discusses the light selection for palmprint recognition through extensive experiments on a large multispectral palmprint database we established (Han et al., 2008).

In general, there are three kinds of popular approaches to palmprint recognition: structural methods (Lin et al., 2005; Liu, 2007), statistical methods (Zhang and Zhang, 2004; Connie et al., 2005; Han, 2004; Ribaric and Fratric, 2005; Wang et al., 2008) and texture coding (Han et al., 2007; Kong and Zhang, 2004; Michael et al., 2008; Zhang et al., 2003) methods. Different approaches focus on different kinds of features. For example, structural methods pay attention to principal lines and wrinkles (Zhang et al., 2003), statistical methods use holistic expression for palmprint recognition, and texture coding schemes assign a feature code for each pixel in the palmprint. Different illumination may enhance different palmprint features as the reflectance and absorbance of human skin relate with spectrum, for example, short wavelength light could enhance the line feature of palms, while long wavelength light could acquire some subcutaneous vein structure (Angelopoulou, 2001). Thus, to get unbiased result for different illuminations, this study employs three different kinds of feature extraction methods, i.e. competitive coding (Kong and Zhang, 2004) (texture coding), wide line detection (Liu, 2007) (structural method), $(2D)^2$PCA (Zhang and Zhou, 2005) (statistical method), to empirically study the light source selection for palmprint recognition.

The rest of this paper is organized as follows. Section 2 describes our data collection. Section 3 briefly introduces the three feature extraction algorithms. Section 4 presents the light source analysis results and Section 5 concludes the paper.

2. Multispectral palmprint data collection

It is known that red, green, and blue are the three primary colors, and the combination of them could result in many different colors in the visible spectrum. We established a multispectral palmprint data collection device which includes the three primary color illumination sources (LED light sources). By using this device we can simulate different illumination conditions. For example, when the red and green LEDs are switched on simultaneously, the yellow like light could be generated. Totally our device could collect palmprint images under seven different color illuminations: red, green, blue, cyan, yellow, magenta and white.

Fig. 1 shows a snapshot of the multispectral palmprint data collection system. It is mainly composed of a monochrome CCD camera, a lens, an A/D converter, a light controller and multispectral light sources. The settings of the lens, A/D converter and CCD camera are identical to the previous palmprint scanning system (Han et al., 2008). The light source is a LED array, where the LEDs are arranged in a circle to provide a uniform illumination. The peak spectrums of red, green, and blue LEDs are 660 nm, 525 nm, and 470 nm respectively. The LED array can switch to different light in 100 ms. The light controller is used to switch on or off the LEDs of different colors. During data collection, the user is asked to put his/her palm on the device for a short time. The device could collect a multispectral palmprint cube, including seven different palm-

Fig. 1. The multispectral palmprint data collection system.

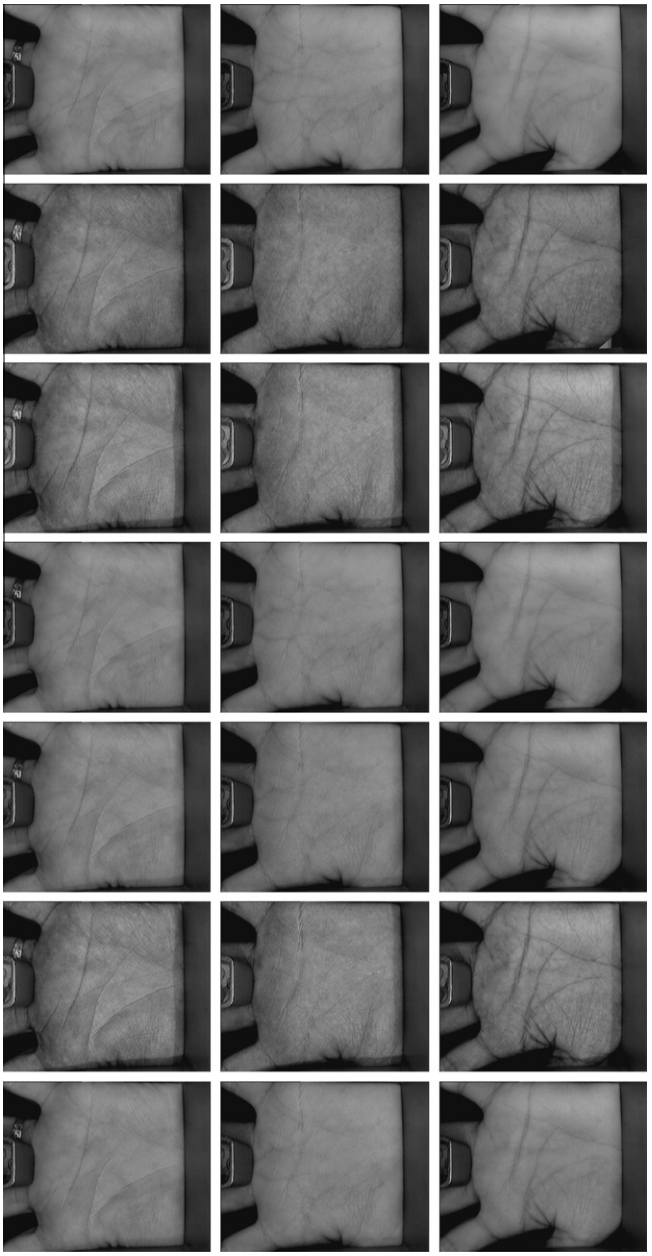

Fig. 2. Sample images of three different palms with different illuminations. Images of each column come from the same palm and are collected by Red, Green, Blue, Yellow, Magenta, Cyan and White illuminations.

print images, in less than 2 s. Fig. 2 shows examples of the collected images under different illuminations.

3. Feature extraction methods

3.1. Wide line detection

A palmprint image has mainly three kinds of features: principal lines (usually three dominant lines on the palm), wrinkles (weaker and more irregular lines) and crease (the ridge and valley structures like in fingerprint) (Zhang et al., 2003). These principal lines and wrinkles could be extracted by a wide line detector directly (Liu, 2007). The thickness of the line is defined as:

$$\begin{aligned} L(x_0,y_0) &= \begin{cases} g - m(x_0,y_0) & \text{if } m(x_0,y_0) < g \\ 0 & \text{otherwise} \end{cases} \\ m(x_0,y_0) &= \sum_{x_0-r\leqslant x\leqslant x_0+r, y_0-r\leqslant y\leqslant y_0+r} c(x,y,x_0,y_0), c(x,y,x_0,y_0) \\ &= \omega_0^* \begin{cases} 0 & \text{if } I(x,y) > I(x_0,y_0) \\ 1 & \text{otherwise} \end{cases} \\ \omega_0 &= \frac{\omega}{\sum_{x_0-r\leqslant x\leqslant x_0+r, y_0-r\leqslant y\leqslant y_0+r}\omega(x,y,x_0,y_0,r)} \text{ and } \omega(x,y,x_0,y_0,r) \\ &= \begin{cases} 1 & \text{if } (x-x_0)^2+(y-y_0)^2 \leqslant r^2 \\ 0 & \text{otherwise} \end{cases} \end{aligned} \tag{1}$$

where g is the geometric threshold, r is radius of the circular mask, and m is the weighed mask having similar brightness. ω is a circular constant weighing mask and ω_0 is the normalization of the circular mask.

To remove noise, a Gaussian smoothing process is employed as a post-processing step. Then the response is binarized after thresholding:

$$\begin{aligned} \widetilde{L}(x,y) &= L(x,y)^* g_\sigma(x,y) \text{ where } g_\sigma(x,y) \\ &= \frac{1}{2\pi\sigma^2}\exp\left(-\frac{x^2+y^2}{2\sigma^2}\right) \end{aligned} \tag{2}$$

$$B(x,y) = \begin{cases} 1 & \text{if } \widetilde{L}(x,y) > t \\ 0 & \text{otherwise} \end{cases} \tag{3}$$

where σ is the scale of the Gaussian filter and t is a threshold. After binarization, the similarity between two palmprints is defined as the proportion of matched bits to the total bits of the two binary palmprint maps (Liu, 2007). As shown in Fig. 3, different parameters will generate different feature maps. In the experiments, we will compute the recognition accuracy on a group of parameters and select the statistical value of each illumination for final comparison.

3.2. Competitive coding

The orientation of palm lines is stable and can serve as distinctive features for personal identification (Kong and Zhang, 2004). To extract the orientation features, six Gabor filters along different orientations ($\theta_i = j\pi/6$, where $j = \{0, 1, 2, 3, 4, 5\}$) are applied to the palmprint image. Here the real part of the Gabor filter is used and it is defined as:

$$\psi(x,y,\omega,\theta) = \frac{\omega}{\sqrt{2\pi}\kappa} e^{-\frac{\omega^2}{8\kappa^2}(4x'^2+y'^2)}\left(e^{i\omega x'} - e^{-\frac{\kappa^2}{2}}\right) \tag{4}$$

where $x' = (x-x_0)\cos\theta + (y-y_0)\sin\theta$, $y' = -(x-x_0)\sin\theta + (y-y_0)\cos\theta$, (x_0, y_0) is the center of the function; ω is the radial frequency in radians per unit length and θ is the orientation of the Gabor functions in radians. κ is defined by $\kappa = \sqrt{2\ln 2}\left(\frac{2^\delta+1}{2^\delta-1}\right)$, where δ is the half-amplitude bandwidth of the frequency response. To reduce the influence of illumination, the direct current is removed from the filter.

By regarding palm lines as the negative lines, the orientation corresponding to the minimal Gabor filtering response (i.e. the negative response but with the highest magnitude) is taken as the feature for this pixel (Kong and Zhang, 2004). Because the contour of Gabor filters is similar to the cross-section profile of palm lines, the higher the magnitude of the response, the more likely there is a line. Since six filters are used to detect the orientation of each pixel, the detected orientation $\{0, \pi/6, \pi/3, \pi/2, 2\pi/3, 5\pi/6\}$ can then be coded by using three bits $\{000, 001, 011, 111, 110, 100\}$ and the Hamming distance is used for comparison between two feature maps (Kong and Zhang, 2004). Fig. 4 shows an example of the extracted orientation feature map, where different gray levels represent different orientation.

3.3. $(2D)^2$PCA

Principal component analysis (PCA) is a widely used statistical analysis method, and $(2D)^2$PCA (Zhang and Zhou, 2005) is an extension of it, which can alleviate much the small sample size problem and better preserve the image local structural information. Suppose we have M subjects and each subject has S sessions in the training data set, i.e. S multispectral palmprint cube were acquired at different times for each subject. Then, we denote by X_{ms}^b (the original image matrix) the bth band image for the mth individual in the sth session. The covariance matrices along the row and column directions are computed as:

$$\begin{aligned} G_1^b &= \frac{1}{MS}\sum_{s=1}^{S}\sum_{m=1}^{M}(X_{ms}^b - \overline{X^b})^T(X_{ms}^b - \overline{X^b}), \\ G_2^b &= \frac{1}{MS}\sum_{s=1}^{S}\sum_{m=1}^{M}(X_{ms}^b - \overline{X^b})(X_{ms}^b - \overline{X^b})^T \end{aligned} \tag{5}$$

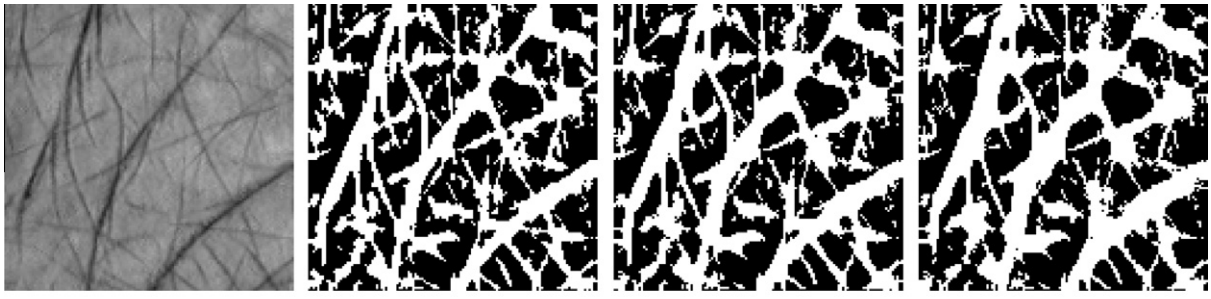

(a) A ROI sample (b) Extracted features by different parameters

Fig. 3. A palmprint ROI (region of interest) sample and its extracted features by wide line detection.

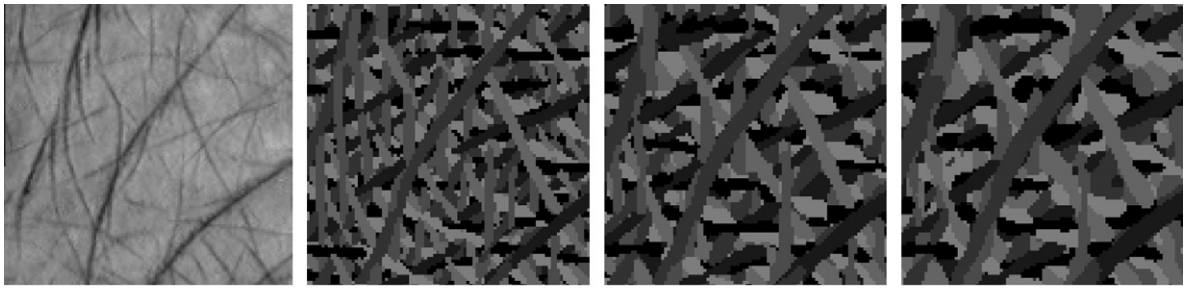

Fig. 4. A ROI sample and its extracted features by competitive coding.

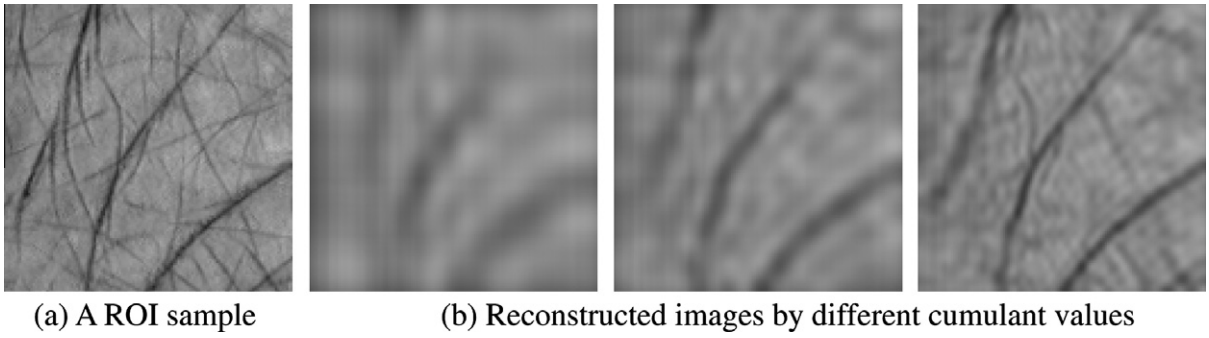

Fig. 5. A ROI sample with its reconstructed images by $(2D)^2$PCA.

where $\overline{X^b} = \frac{1}{MS}\sum_{s=1}^{S}\sum_{m=1}^{M} X_{ms}^b$.

The project matrix $V_1^b = [v_{11}^b, v_{12}^b, \ldots, v_{1k_1^b}^b]$ is composed of the orthogonal eigenvectors of G_1^b corresponding to the k_1^b largest eigenvalues, and the projection matrix $V_2^b = [v_{21}^b, v_{22}^b, \ldots, v_{2k_2^b}^b]$ consists of the orthogonal eigenvectors of G_2^b corresponding to the largest k_2^b eigenvalues. k_1^b and k_2^b can be determined by setting a threshold to the cumulant eigenvalues:

$$\sum_{j_c=1}^{k_1^b} \lambda_{1j_c}^b \Big/ \sum_{j_c=1}^{I_c} \lambda_{1j_c}^b \geqslant C_u,\ \sum_{j_r=1}^{k_2^b} \lambda_{2j_c}^b \Big/ \sum_{j_r=1}^{I_r} \lambda_{2j_c}^b \geqslant C_u \tag{6}$$

where $\lambda_{11}^b, \lambda_{12}^b, \ldots, \lambda_{1I_c}^b$ are the first I_c biggest eigenvalues of G_1^b, $\lambda_{21}^b, \lambda_{22}^b, \ldots, \lambda_{2I_r}^b$ are the first I_r biggest eigenvalues of G_2^b, and C_u is a pre-set threshold. For each given band bth, the test image T^b is projected to T^b by V_1^b and $V_2^b(V_2^{bT} \times T^b \times V_1^b)$, then Euclidean distance is used to measure the dissimilarity (Zhang and Zhou, 2005). Fig. 5 shows the reconstructed image $(V_2^b \times T^b \times V_1^{bT})$ by different C_u.

4. Analyzes of light source selection

4.1. Database description

We collected multispectral palmprint images from 250 subjects using the developed data acquisition device. The subjects were mainly volunteers from our institutes. In the database, 195 subjects are male and the age distribution is from 20 to 60 years old. We collected the multispectral palmprint images on two separate sessions. The average time interval between the two occasions is 9 days. On each session, the subject was asked to provide six samples of each of his/her left and right palms. So our database contains 6000 images for each band from 500 different palms. For each shot, the device collected seven images from different bands (red, green, blue, cyan, yellow, magenta, and white) in less than two seconds. In palmprint acquisition, the users are asked to keep their palms stable on the device. The resolution of the images is $352 * 288$ (<100 dpi).

After obtaining the multispectral cube, a local coordinate of the palmprint image is established (Zhang et al., 2003) from the blue band, and then a ROI is cropped from each band based on the local coordinate. For the convenience of analysis, we normalized these ROIs to a size of $128 * 128$. To remove the global intensity and contrast effect (Zuo et al., 2006), all images are normalized to have a mean of 128 and standard deviation of 20.

4.2. Palmprint verification results by wide line detection

To compute the verification accuracy, each palmprint image is matched with all the other palmprint images in the database. A match is counted as a genuine if the two palmprint images are from the same palm; otherwise, it is counted as an impostor. The total number of matches is 17,997,000 and the number of genuine is 33,000. The Equal Error Rate (EER) (the point when False Accept Rate (FAR) is equal to False Reject Rate (FRR)) is used to evaluate the accuracy.

As discussed in Section 3.1, there are four parameters which could influence the feature extraction, r, t, g, and σ. To reduce the possible parameter space, we fixed $g = 0.5$ and $t = 0.1$ (Liu, 2007), and selected nine different values for r ([12, 20]) and six different values ([0.75, 2]) for σ, because these values could include optimal parameters (Liu, 2007). Thus, the total number of test settings is 54. The EER under different settings with different illuminations are plotted in Fig. 6 and the statistical values of EER for each light are listed in Table 1.

4.3. Palmprint verification results by competitive coding

As discussed in Section 3.2, parameters ω and δ could influence the extracted features. We selected 20 different values for ω

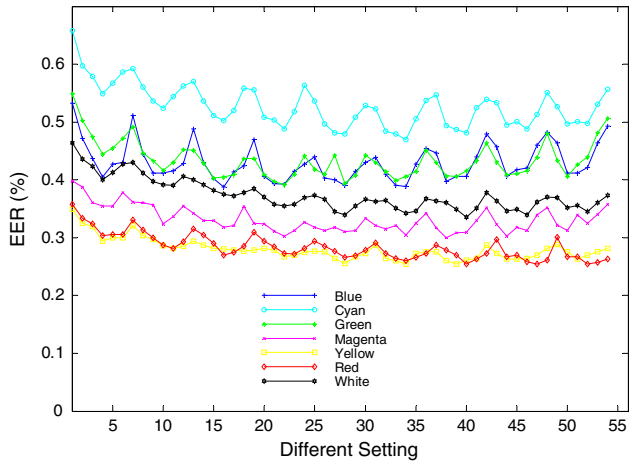

Fig. 6. EER values under different settings by wide line detection.

([4.0, 5.9]) and 15 different values for δ ([1, 1.7]) because these values could cover optimal parameters (Zhang et al., 2010), and we used the same test protocol as discussed in Section 4.2. Thus, the total number of test settings is 300. The EER under different setting with different illuminations are plotted in Fig. 7 and the statistical values of EER for each light are listed in Table 2.

4.4. Palmprint identification results by $(2D)^2PCA$

In this section, identification instead of verification is implemented. The whole database is partitioned into two parts, training set and test set. The training set is used to estimate the projection matrix and is taken as gallery samples. The test samples are matched with the training samples and nearest neighborhood classification is employed. The ratio of the number of correct matches to the number of test samples, i.e. the recognition accuracy, is used as the evaluation criteria. To reduce the dependency of experimental results on training sample selection, we designed the experiments as follows. Firstly, the first three samples in the first session are chosen as training set and the remaining samples are used as test set. Secondly, the first three samples in the second session are chosen as training set, and the remaining samples are used as test set. Finally, the average accuracy is computed.

As shown in Section 3.3, there is only one parameter, C_u, to control the feature extraction. The accuracies under different settings with different illuminations are plotted in Fig. 8 and the highest accuracy for each light is listed in Table 3.

4.5. Discussions

From Figs. 6–8 and Tables 1–3, we could have three findings. First, no spectrum could compete with all the others for all settings. This is mainly because different light could enhance different

Table 1
Statistical values of EER for each color by wide line detection.

	Blue	Cyan	Green	Magenta	Yellow	Red	White
Mean	0.4306	0.5275	0.4344	0.3318	0.2798	0.2839	0.3738
Standard deviation	0.0328	0.0370	0.0319	0.0221	0.0185	0.0224	0.0278

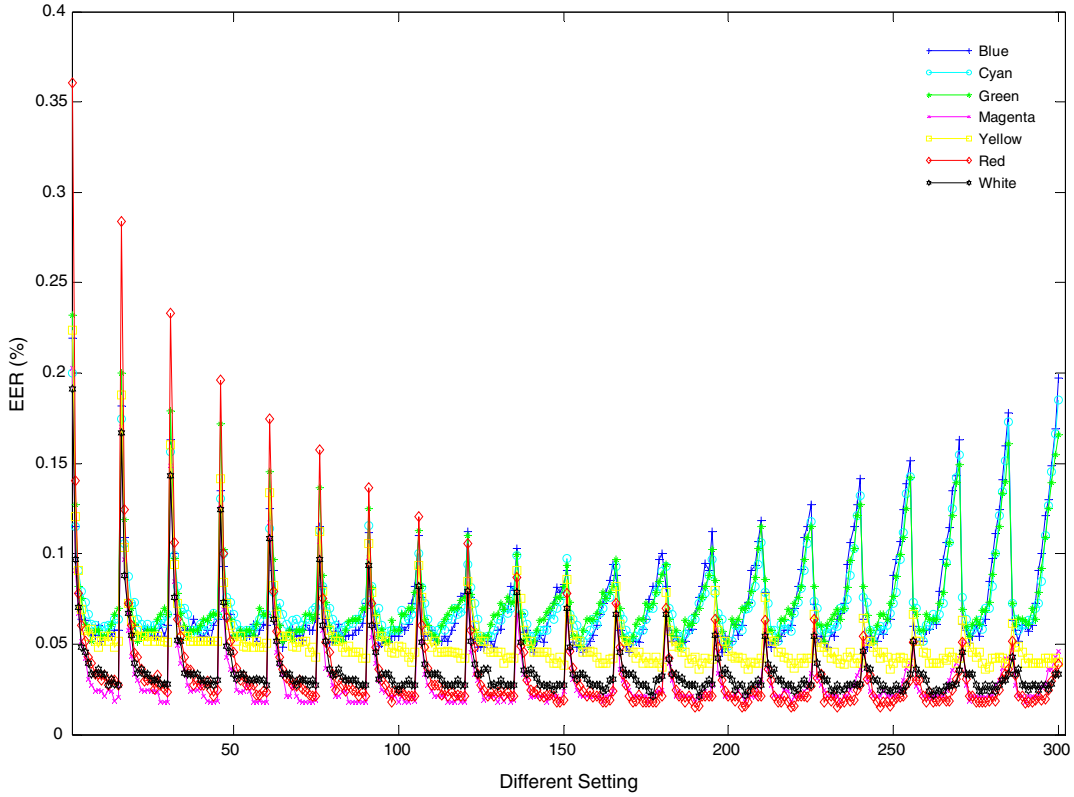

Fig. 7. EER values under different settings by competitive coding.

Table 2
Statistical values of EER for each color by competitive coding.

	Blue	Cyan	Green	Magenta	Yellow	Red	White
Mean	0.0718	0.0733	0.0742	0.0305	0.0523	0.0351	0.0358
Standard deviation	0.0288	0.0243	0.0262	0.0220	0.0204	0.0358	0.0195

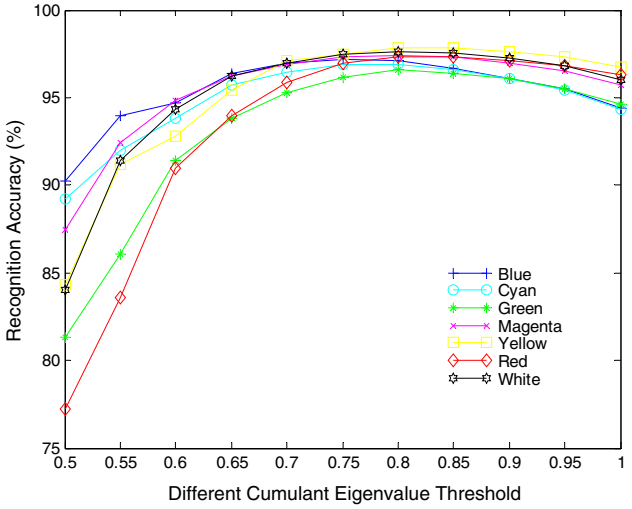

Fig. 8. Recognition Accuracy under different C_u by $(2D)^2PCA$.

Table 3
The highest accuracy for each color by $(2D)^2PCA$.

Blue	Cyan	Green	Magenta	Yellow	Red	White
97.2000	96.8777	96.6334	97.4333	97.8777	97.3555	97.6334

features of palms, while these different features have different intensity distributions which are in favor of different parameters.

Second, among the three primary colors, red leads to a little higher accuracy than blue and green. This is mainly because red could not only capture most of the palm line information, but also capture some palm vein structures as shown in Fig. 2. This additional palm vein information helps in classifying those palms with similar palm lines. It could also explain why the composite colors (magenta, yellow, white) could get better accuracy than cyan.

Last, white color could not get the best accuracy among the seven spectra. Yellow achieves the best result by the schemes of wide line detection and $(2D)^2PCA$, while magenta achieves the best result by the scheme of competitive coding. Furthermore, there is a statistically significant difference at a significance level of 0.05 between magenta and white in competitive coding trails, and between yellow and white in wide line detection trials. This finding could be explained as follows.

According to additive color mixing and object imaging formula (Kittler and Sadeghi, 2004), the intensity of palmprint image by white light could be regarded as a composition of three components, intensity by blue light, green light and red light. As shown in Fig. 2, the palmprint images under blue and green illumination are more similar to each other than to the image under red illumination. A quantitative image similarity index, CW-SSIM, (Wang and Simoncelli, 2005) further validate that blue and green collect much redundant information, as the average similarity between blue and green is 0.95 (the maximal value is 1), while the average similarity between blue and red, and green and red are 0.83. The redundancy makes white color fail to capture more information than the yellow or magenta color, and sometimes the accuracy drops a little. This is also consistent with the finding of Fratric and Ribaric (2008), fusion of blue and red channels gets better result than fusion of three channels.

5. Conclusion

Palmprint recognition has been attracting lots of research attention in the past decade and many data collection devices have been proposed. In order for good image quality and high data capture speed, using cameras mounted with active lighting sources is the most popular device configuration. Almost all existing devices used white light as the illumination source but there was no systematic analysis on whether the white light is the optimal light source for palmprint recognition. This paper made such an effort on answering this problem by establishing a large multispectral palmprint database using our developed device. With the database we empirically evaluated the recognition accuracies of palmprint images under seven different colors by three different methods. Our experimental results showed that the white color is not the optimal color for palmprint recognition and the yellow or magenta color could achieve higher accuracy than the white color.

However, so far our data were collected from East Asian residents (more specifically Chinese) only. Since the palm spectral properties of different groups may be different (Angelopoulou, 2001), the finding of this work may not valid for other groups. In the future, more samples from other groups will be collected to investigate the best illumination conditions for palmprint recognition.

Acknowledgements

The work is partially supported by the GRF fund from the HKSAR Government (PolyU 5351/08E), the central fund from Hong Kong Polytechnic University, Key Laboratory of Network Oriented Intelligent Computation (Shenzhen), the Natural Scientific Research Innovation Foundation in Harbin Institute of Technology, Henan Provincial Fund (No. 092300410154), the Natural Science Foundation of China (NSFC) (Nos. 60803090 and 61020106004). The authors also would like thank for Dr. Qin Li in the Henan Provincial Key Lab on Information Network, Zhengzhou University, Zhengzhou, Henan, China for profitable discussions.

References

Angelopoulou, E., 2001. Understanding the color of human skin. Proc. SPIE Conf. on Human Vision and Electronic Imaging, vol. 4299. SPIE, pp. 243–251.
Connie, T., Jin, A.T.B., Ong, M.G.K., Ling, D.N.C., 2005. An automated palmprint recognition system. Image Vision Comput. 23, 501–515.
Duta, N., Jain, A.K., Mardia, K.V., 2002. Matching of palmprint. Pattern Recognition Lett. 23, 477–485.
Fratric, I., Ribaric, S., 2008. Colour-based palmprint verification – An experiment. In The 14th IEEE Mediterranean Electrotechnical Conference, pp. 890–895.
Guo, Z., Zhang, D., Zhang, L., 2009. Is white light the best illumination for palmprint recognition. In: Internat. Conf. on Computer Analysis of Images and Patterns, pp. 50–57.
Han, C., 2004. A hand-based personal authentication using a coarse-to-fine strategy. Image Vision Comput. 22, 909–918.
Han, D., Guo, Z., Zhang, D., 2008. Multispectral palmprint recognition using wavelet-based image fusion. In: Internat. conf. on signal processing, pp. 2074–2077.
Han, Y., Sun, Z., Wang, F., Tan, T., 2007. Palmprint recognition under unconstrained scenes. In: Asian Conf. Computer Vision. LNCS, vol. 4844, pp. 1–11.
Jain, A., Bolle, R., Pankanti, S., 1999. Biometrics: Personal Identification in Network Society. Kluwer Academic Publishers, Boston.

Kittler, J., Sadeghi, M.T., 2004. Physics-based decorrelation of image data for decision level fusion in face verification. In: Multiple Classifier Systems. LNCS, vol. 3077, pp. 354–363.
Kong, A., Zhang, D., 2004. Competitive coding scheme for palmprint verification. In: Internat. Conf. on Pattern Recognition, pp. 520–523.
Kong, A., Zhang, D., Kamel, M., 2009. A survey of palmprint recognition. Pattern Recognition 42, 1408–1418.
Kumar, A., Wong, D.C.M., Shen, H., Jain, A.K., 2003. Personal verification using palmprint and hand geometry biometric. In: Proc. AVBPA, pp. 668–675.
Lin, C., Chuang, T., Fan, K., 2005. Palmprint verification using hierarchical decomposition. Pattern Recognition 38, 2639–2652.
Liu, L., 2007. Wide line detector and its applications. Ph. D thesis, the Hong Kong Polytechnic University.
Michael, G.K.O., Connie, T., Teoh, A.B.J., 2008. Touch-less palm print biometrics: Novel design and implementation. Image Vision Comput. 26, 1551–1560.
Ribaric, S., Fratric, I., 2005. A biometric identification system based on Eigenpalm and Eigenfinger features. IEEE Trans. Pattern Anal. Machine Intell. 27, 1698–1709.
Wang, J.-G., Yau, W.-Y., Suwandy, A., Sung, E., 2008. Person recognition by fusing palmprint and palm vein images based on "Laplacianpalm" representation. Pattern Recognition 41, 1514–1527.
Wang, Z., Simoncelli, E.P., 2005. Translation insensitive image similarity in complex wavelet domain. IEEE Iinternat. Conf. on Acoustics, Speech, and Signal Processing, pp. 573–576.
Wong, M., Zhang, D., Kong, W.-K., Lu, G., 2005. Real-time palmprint acquisition system design. IEE Proc.-Vision Image Signal Process 152, 527–534.
Wu, J., Qiu, Z., Sun, D., 2008. A hierarchical identification method based on improved hand geometry and regional content feature for low-resolution hand images. Signal Process. 88, 1447–1460.
Zhang, D., Guo, Z., Lu, G., Zhang, L., Zuo, W., 2010a. An online system of multispectral palmprint verification. IEEE Trans. Instrum. Meas. 59, 480–490.
Zhang, D., Kong, W., You, J., Wong, M., 2003. Online palmprint identification. IEEE Trans. Pattern Anal. Machine Intell. 25, 1041–1050.
Zhang, D., Shu, W., 1999. Two novel characteristics in palmprint verification: Datum point invariance and line feature matching. Pattern Recognition 32, 691–702.
Zhang, D., Zhou, Z., 2005. $(2D)^2$ PCA: 2-directional 2-dimensional PCA for efficient face representation and recognition. Neurocomputing 69, 224–231.
Zhang, L., Zhang, D., 2004. Characterization of palmprints by wavelet signatures via directional context modeling. IEEE Trans. Systems Man Cybernet. Part B 34, 1335–1347.
Zhang, L., Zhang, L., Zhang, D., Zhu, H.L., 2010b. On-line finger-knuckle-print verification for personal authentication. Pattern Recognition 43 (7), 2560–2571.
Zuo, W., Zhang, D., Wang, K., 2006. An assembled matrix distance metric for 2DPCA-based image recognition. Pattern Recognition Lett. 27, 210–216.